Article

Neuron

# Nonlinear Spatiotemporal Integration by Electrical and Chemical Synapses in the Retina

## Highlights

- Gap junctions mediate lateral interactions across parallel ON bipolar cell circuits
- These lateral interactions nonlinearly shape glutamate release from bipolar cells
- Bipolar cell synaptic output is preferentially enhanced for low contrast stimuli
- Nonlinear lateral interactions increase retinal ganglion cell sensitivity to motion

## Authors

Sidney P. Kuo, Gregory W. Schwartz, Fred Rieke

## Correspondence

rieke@u.washington.edu

## In Brief

Kuo et al. find that electrical and chemical synaptic transmission work in concert to control glutamate release from retinal ON cone bipolar cells. This interaction enhances retinal ganglion cell sensitivity to visual inputs with strong spatiotemporal correlations, such as motion.

Kuo et al., 2016, Neuron *90*, 320–332
April 20, 2016 
http://dx.doi.org/10.1016/j.neuron.2016.03.012

CellPress

CellPress

Neuron
Article

# Nonlinear Spatiotemporal Integration by Electrical and Chemical Synapses in the Retina

Sidney P. Kuo,[1] Gregory W. Schwartz,[1,2] and Fred Rieke[1,*]
[1]Department of Physiology and Biophysics and Howard Hughes Medical Institute, University of Washington, Seattle, WA 98195, USA
[2]Present address: Departments of Ophthalmology and Physiology, Northwestern University, Chicago, IL 60611, USA
*Correspondence: rieke@u.washington.edu
http://dx.doi.org/10.1016/j.neuron.2016.03.012

## SUMMARY

**Electrical and chemical synapses coexist in circuits throughout the CNS. Yet, it is not well understood how electrical and chemical synaptic transmission interact to determine the functional output of networks endowed with both types of synapse. We found that release of glutamate from bipolar cells onto retinal ganglion cells (RGCs) was strongly shaped by gap-junction-mediated electrical coupling within the bipolar cell network of the mouse retina. Specifically, electrical synapses spread signals laterally between bipolar cells, and this lateral spread contributed to a nonlinear enhancement of bipolar cell output to visual stimuli presented closely in space and time. Our findings thus (1) highlight how electrical and chemical transmission can work in concert to influence network output and (2) reveal a previously unappreciated circuit mechanism that increases RGC sensitivity to spatiotemporally correlated input, such as that produced by motion.**

## INTRODUCTION

Diverse neural circuits use a combination of electrical and chemical synapses to convey signals between neurons (reviewed in Pereda, 2014). Electrical synapses often spread signals laterally among populations of functionally related cells (Christie and Westbrook, 2006; Detwiler and Hodgkin, 1979; DeVries et al., 2002; Galarreta and Hestrin, 2001; Schwartz, 1976; Trenholm et al., 2013a; Veruki and Hartveit, 2002a, 2002b; Vervaeke et al., 2012). Such lateral spread could have an important influence upon neurotransmitter release from electrically coupled networks (Attwell and Wilson, 1980). For example, because release of neurotransmitter depends nonlinearly on presynaptic membrane potential (Katz and Miledi, 1967), even relatively weak electrical coupling could result in substantial modulations in synaptic output to postsynaptic targets. Yet few studies have shown how electrical and chemical synapses work together to determine network output. Here, we took advantage of the anatomical organization and experimental accessibility of the mouse retina to examine how electrical coupling influences synaptic output from retinal bipolar cells in response to spatiotemporally patterned light stimuli.

Visual space is represented explicitly in the basic organization of the feed-forward circuits that convey excitatory signals from cone photoreceptors to RGCs, the output neurons of the retina. In the outer retina, a regularly spaced array of cones transduces light into electrical signals and releases glutamate onto the dendrites of cone bipolar cells. Cone bipolar cells subsequently transmit light-initiated signals to the inner retina, where they form glutamatergic synapses upon the dendrites of RGCs. Each of the ~12 distinct subtypes of cone bipolar cells tile visual space (i.e., their axons and dendrites occupy adjacent, mostly non-overlapping regions of retina) (Wässle et al., 2009; Helmstaedter et al., 2013). A RGC receives glutamatergic synaptic input from up to several hundred cone bipolar cells, sometimes comprising predominantly one bipolar subclass (Freed and Sterling, 1988; Schwartz et al., 2012). Hence, excitatory synaptic input to a RGC generally reflects the combined influence of a large population of bipolar cells, with synapses upon distinct portions of the dendrite relaying information about specific regions in the visual field (Figure 1B). The RGC receptive field depends on how signals traversing these parallel pathways are integrated (reviewed in Gollisch and Meister, 2010; Schwartz and Rieke, 2011).

Importantly, extensive electrical networks in both the outer and inner retina extend laterally across the cone bipolar circuits that converge upon RGCs (Figure 1A). In the outer retina, gap junctions form electrical synapses among the axons of neighboring rods, between rods and cones, and among cones (Asteriti et al., 2014; DeVries et al., 2002; Tsukamoto et al., 2001). In the mammalian inner retina, the axon terminals of most or all subtypes of ON cone bipolar cells are coupled via gap junctions with the dendrites of AII amacrine cells (Cohen and Sterling, 1990; Marc et al., 2014; Veruki and Hartveit, 2002a) or via gap junctions directly between cone bipolar cells (Cohen and Sterling, 1990). The extensive coupling between AII amacrine and ON cone bipolar cells suggests that signals initiated by cone input to the dendrites of one cone bipolar cell can spread laterally to neighboring bipolar cells. Consistent with this, the excitatory receptive fields of bipolar cells can be more than twice as large as expected from the anatomical dimensions of their dendrites (Berntson and Taylor, 2000; Dacey et al., 2000; Schwartz et al., 2012).

We sought to understand whether and how lateral interactions mediated by electrical synapses influence the synaptic output of cone bipolar cell circuits upstream of ON RGCs. Nonlinear transformation of visual signals by bipolar cell synapses has previously been identified as a key step in retinal computation (Asari

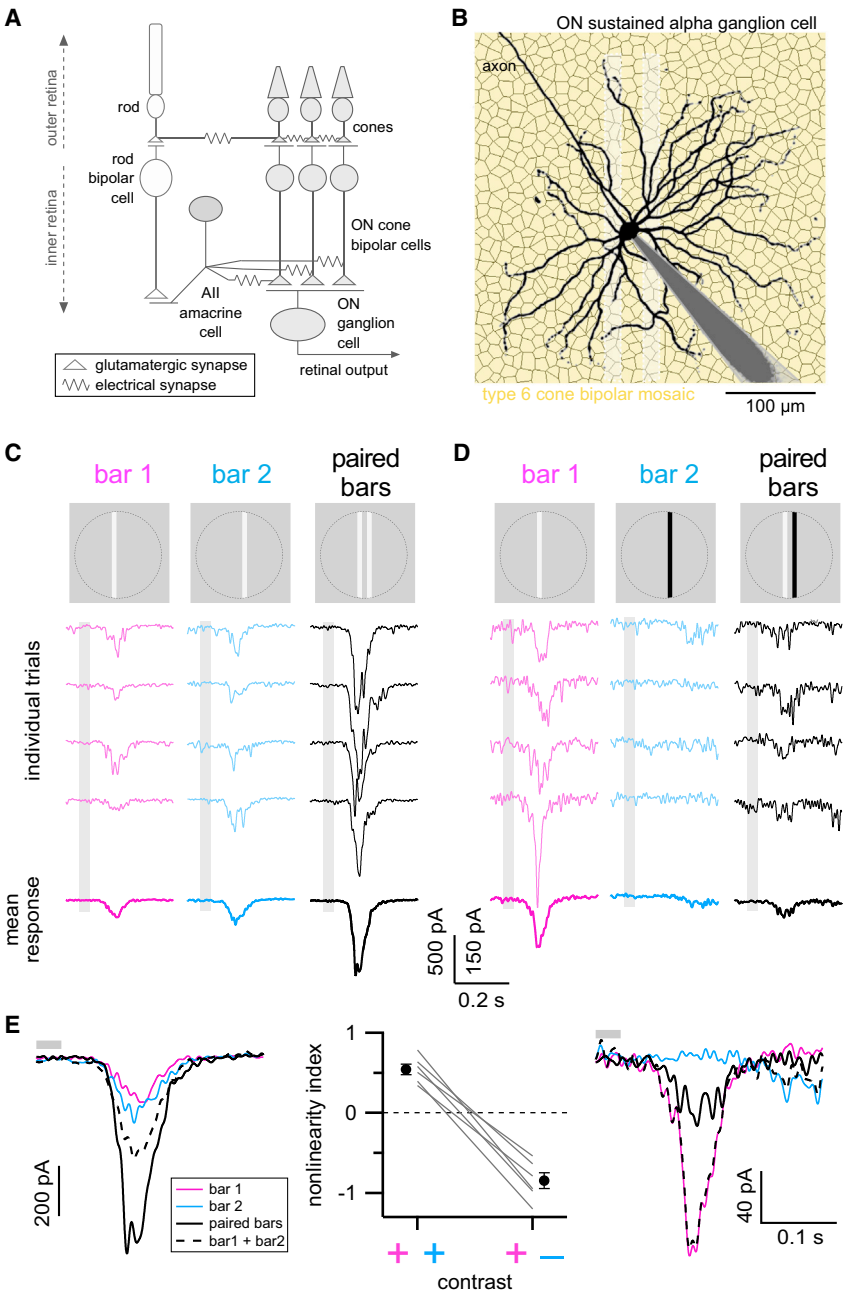


**Figure 1. Paired Stimuli Reveal Nonlinear Lateral Interactions**

(A) Simplified diagram of chemical and electrical synapses in the excitatory ON circuitry of the retina.

(B) Dye-filled ON-S ganglion cell (black; gray shading is patch-pipette) over a simulated mosaic of type 6 cone bipolar cells (yellow hexagons) to illustrate that RGC dendrites receive convergent input from numerous parallel feed-forward bipolar circuits. Shaded white rectangles show dimensions of the paired bar stimulus used in the following experiments.

(C and D) Example responses to positive contrast (C) or positive and negative contrast bars (D). Top row, light stimulus. Middle rows, example single trial responses to single or paired bar stimuli. Bottom row, mean responses (eight trials each). Responses in (C) and (D) are from same example cell. Stimulus timing (33 ms flash) is indicated by light gray boxes.

(E) Overlaid average responses from (C) (left) and (D) (right). Dashed black lines show linear sum of single bar responses (colored traces). Solid black lines show measured paired bar response. Summary of nonlinear indices for responses to paired positive contrast bars or paired positive/negative contrast bars shown in middle panel. Gray lines are data from individual cells and filled black circles show mean ± SEM (n = 6 cells). Gray bars above traces show stimulus timing. All bars were 18 µm wide, inter-bar spacing 18–22 µm. See also Figure S1.

and Meister, 2012; Baccus et al., 2008; Chang and He, 2014; Demb et al., 2001; Grimes et al., 2014; Grimes et al., 2015). Here, we tested the hypothesis that the gap-junction-mediated lateral spread of signals across bipolar cell pathways upstream of this synaptic nonlinearity could enhance retinal sensitivity to visual inputs that elicit overlapping lateral and feed-forward signals within the bipolar network.

## RESULTS

The experiments described below show that (1) lateral interactions nonlinearly influence bipolar cell synaptic output, (2) these interactions arise from a combination of gap-junction-mediated signal spread and nonlinear synaptic output from bipolar cells, and (3) lateral interactions enhance RGC sensitivity to stimuli with strong spatiotemporal correlations.

### Nonlinear Integration in the ON Bipolar Cell Network

We performed all experiments except those in Figures 3A–3D using a flat mount preparation of the isolated mouse retina. Whole-cell voltage-clamp recordings measured excitatory synaptic inputs to RGCs while spatially distinct subsets of presynaptic bipolar cells were probed with narrow bars of light. We focused primarily on a specific RGC subtype, ON sustained alpha ganglion cells (ON-S RGCs), because previous work demonstrated that these cells receive the majority of their excitatory synaptic input (>70%) from a single subtype of bipolar cell (type 6; Schwartz et al., 2012). Thus, excitatory synaptic currents to ON-S RGCs provided a sensitive measure of the combined synaptic output from a population of several hundred presynaptic bipolar cells, and these bipolar cells have limited dendritic or axonal overlap due to the tiling of individual bipolar types (see Figure 1B).

We used a simple set of visual stimuli to determine whether lateral interactions can influence ON cone bipolar cell output (Figure 1C, top row). Narrow, positive contrast (luminance increment

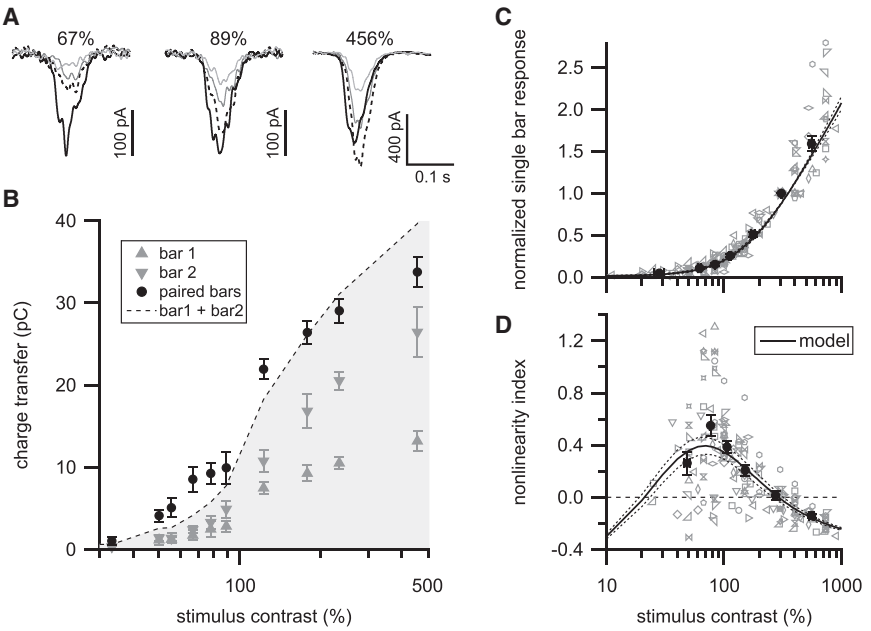


**Figure 2. Nonlinear Interaction Depends on Stimulus Contrast**

(A) Mean excitatory currents in response to single (gray) or paired (black) bar presentations at different stimulus contrasts in an example ON-S RGC. Dashed lines shows sum of single bar responses.

(B) Contrast-response relationship for same cell shown in (A). Symbols and error bars show mean ± SEM. Filled black circles that fall above (within) the grayed area indicate supralinear (sublinear) interactions.

(C) Population summary of single bar contrast-response relationship. Gray symbols show data from individual cells. Filled circles with error bars are mean ± SEM across cells (n = 19 cells) for data collected into approximately equal sized bins by contrast. Responses were normalized to the response at 315%–450% contrast. Solid black curve and dotted lines show mean and SEM, respectively, of bipolar population model output (see Figure 5 and associated text; *xhalf* = 71 ± 9% contrast, $h = 2.18 \pm 0.16$, $\sigma_{bipolar} = 14 \pm 2\%$ contrast).

(D) Population summary of nonlinearity index versus stimulus contrast for same cells shown in (C). Line styles and symbols same as in (C). See also Figures S2, S4, and S5.

above background) bars of light were briefly flashed at one spatial location ("bar 1"; Figure 1C, left), at a different location ("bar 2"; Figure 1C, middle), or at both locations simultaneously ("paired bars"; Figure 1C, right). The width of the bars (18 μm) spanned the dendrites of a single type 6 bipolar cell (~15–17 μm diameter; Dunn and Wong, 2012; Wässle et al., 2009), and the bar spacing meant that the different bars provided direct dendritic input to distinct subsets of bipolar cells (18–22 μm in Figure 1). We systematically varied bar spacing in a subsequent experiment (see Figures 6A and 6B). Because our goal was to examine whether electrical interactions among local bipolar networks affect bipolar output, we limited potential influences from the ganglion cell receptive field surround (Farrow et al., 2013) by restricting all stimuli to a 360 μm diameter circular region centered on the ganglion cell soma. This area approximates the extent of the receptive field center of ON-S RGCs (Bleckert et al., 2014).

If bipolar cells across the receptive field of an ON-S RGC integrate signals linearly, then the response to the paired bar stimulus should equal the linear sum of the single bar presentations. Excitatory currents measured in response to the paired bar stimulus, however, exceeded the linear sum of the single bar responses (Figure 1E, left). Further, if a negative contrast bar was used at one of the bar positions, responses to paired bars were smaller than the linear sum of the single bar responses (Figure 1E, right).

We quantified nonlinear summation using a nonlinearity index (*NLI*) defined as

$$NLI = \frac{R_{both} - (R_{bar1} + R_{bar2})}{R_{bar1} + R_{bar2}},$$

where $R_{bar1}$, $R_{bar2}$, and $R_{both}$ are the integrated responses to bar 1, bar 2, and the paired bars; positive NLI values indicate a supralinear interaction, negative values indicate sublinear interactions, and a value of zero indicates purely linear interactions. Paired positive contrast bars consistently produced supralinear interactions (NLI = 0.54 ± 0.07; n = 6 cells, mean ± SEM), whereas paired bars with opposite contrast polarities resulted in sublinear interactions in the same cells (NLI = −0.85 ± 0.10) (Figure 1E).

We also adjusted bar intensity to determine whether nonlinear integration depends on stimulus strength. For simplicity, we focused on positive contrast stimuli in these and subsequent experiments. Paired positive contrast bars produced strongly supralinear responses at low stimulus strengths (maximal NLI at ~70% stimulus contrast), but supralinear integration progressively declined with increasing stimulus contrast until interactions became sublinear at high stimulus contrasts (Figure 2). Thus, supralinear integration was specifically restricted to those stimulus contrasts that elicited small single bar responses. This finding is consistent with an important role for nonlinear synaptic output from bipolar cells in supralinear integration (see below).

The excitatory currents that we recorded using voltage-clamp should reflect nonlinear integration in the presynaptic bipolar network. But voltage-clamp errors could permit postsynaptic factors, such as nonlinear dendritic integration or poorly clamped inhibitory conductances, to contribute to the observed responses (Williams and Mitchell, 2008). However, control experiments in which we compared single and paired bar responses at several dendritic locations (Figure S1) argue against a postsynaptic contribution to the supralinear paired bar responses we measured in ON-S RGCs.

These experiments indicate that retinal responses to stimuli in different spatial locations interact nonlinearly to control the synaptic output of the ON cone bipolar network. This finding is consistent with lateral signal spread through gap junctions influencing bipolar cell presynaptic membrane potential, and thereby modulating bipolar cell synaptic output. Our next experiments tested this hypothesis.

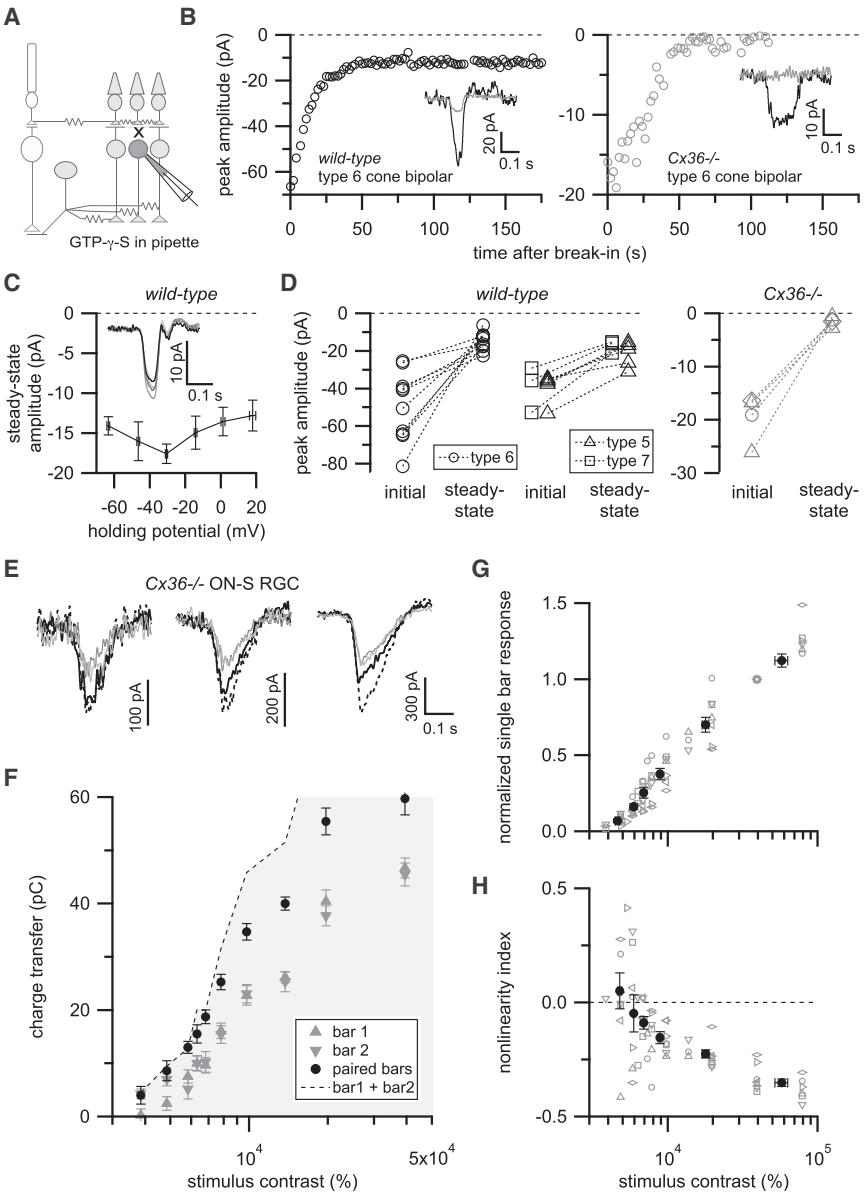


**Figure 3. Gap Junctions Contribute to Supralinear Paired Bar Integration**

(A) Schematic illustration of experiment in (B)–(D) to isolate gap-junction-mediated input to ON cone bipolar cells.

(B) Example response time courses for type 6 bipolar cell in wild-type (left) or *Cx36*$^{-/-}$ (right) retina when GTP-γ-S was included in the pipette solution. Saturating flashes (10 ms; 520-μm diameter circular spot) were presented every 2 s after achieving whole-cell configuration. Insets show example single trial responses immediately after break-in (black trace) or once responses had reached a steady-state level (gray).

(C) Summary of peak flash responses in ON cone bipolar cells at different holding potentials >2 min after dialysis with GTP-γ-S (n=4 cells; two type 6 bipolar, one each type 5 and type 7 bipolar cells; error bars show SEM). Inset shows mean flash responses from example type 6 bipolar cell held at −64 (darkest trace) to +16 mV (lightest).

(D) Comparison of initial versus steady-state ON cone bipolar responses with GTP-γ-S in recording pipette in wild-type (left) or *Cx36*$^{-/-}$ mice (right). Diamonds for *Cx36*$^{-/-}$ data represent a recording from an unknown ON bipolar type. Other symbols follow legend for wild-type recordings. Recordings shown in (B)–(D) acquired in a retinal slices. In these experiments, NBQX (10 μM) was included in bath solutions to eliminate rod bipolar pathway-mediated signals.

(E) Example single (gray) and paired (black) bar responses at different stimulus contrasts from example ON-S RGC in *Cx36*$^{-/-}$ retina (flat mount). Stimulus contrasts (left to right): 5,820%, 7,790%, and 19,600%.

(F) Contrast-response relationship for cell shown in (E). Symbols show mean ± SEM.

(G) Summary of single bar responses for ON-S RGCs recorded in *Cx36*$^{-/-}$ mice. Gray symbols are data from single cells; filled circles are mean ± SEM (n = 7 cells).

(H) Summary of nonlinearity index versus stimulus contrast. Same symbol and color scheme as (G). Note different contrast scale in (F)–(H) compared to Figures 2B–2D. See also Figure S3.

## Gap Junctions Contribute to ON Cone Bipolar Cell Light Responses

Previous observations that ON cone bipolar cells can respond to light stimuli ~20–30 μm beyond the outermost extent of their dendrites provides indirect evidence that gap junctions can spread signals laterally within the ON cone bipolar cell network (Berntson and Taylor, 2000; Dacey et al., 2000; Schwartz et al., 2012). We sought to more directly determine whether gap junctions contribute to ON cone bipolar cell light responses. To do this, we made recordings from ON cone bipolar cells that were dialyzed via the patch pipette with GTP-γ-S, a poorly hydrolyzable GTP analog (Figure 3A). The dendrites of ON bipolar cells use metabotropic glutamate receptors (mGluR6) to detect glutamate release from cone photoreceptor terminals (Nakajima et al., 1993; Slaughter and Miller, 1981); introduction of GTP-γ-S eliminates the intrinsic light response of ON bipolar cells by interfering with the G protein signaling cascade downstream of mGluR6 activity (Nawy and Jahr, 1990; Sampath and Rieke, 2004; Shiells and Falk, 1990). Indeed, saturating flash responses of ON cone bipolar cells rapidly declined after establishing whole-cell recordings with GTP-γ-S in the pipette solution (Figure 3B, left). However, unlike rod bipolar cells, in which flash responses are completely eliminated by intracellular GTP-γ-S (Sampath and Rieke, 2004), a prominent GTP-γ-S-insensitive component of the flash response remained in all ON cone bipolar cells tested (Figure 3D, left; GTP-γ-S-insensitive component = 35.8 ± 6.6% of initial response; n = 10 type 6 bipolar cells).

Importantly, the light responses of non-recorded bipolar cells should remain intact with the intracellular GTP-γ-S manipulation (see Figure 3A). Thus, the GTP-γ-S-insensitive response likely reflects a contribution from light responses of nearby ON cone bipolar cells conveyed via electrical synapses in the

inner retina. We tested this idea in two ways. First, we measured flash responses in GTP-γ-S-dialyzed bipolar cells at several different membrane holding potentials. Gap-junction-mediated conductances between AII amacrine cells and ON cone bipolar cells do not exhibit clear voltage-dependence over a wide range of transjunctional voltages (Veruki and Hartveit, 2002a). The amplitude and polarity of gap-junction-mediated currents should therefore not depend strongly on holding potential. Indeed, GTP-γ-S-insensitive currents were not significantly affected when bipolar cells were clamped at different membrane voltages (Figure 3C). Second, we measured light responses in ON cone bipolar cells from mice lacking the gene coding for connexin36 (GJD2; *Cx36*$^{-/-}$ or *Gjd2*$^{-/-}$ mice), which is required for electrical synapses between AII amacrine cells and ON cone bipolar cells (Deans et al., 2002). Unlike results from wild-type mice, flash responses were almost completely suppressed by GTP-γ-S in ON cone bipolar cells recorded from *Cx36*$^{-/-}$ mice (Figures 3B and 3D right; GTP-γ-S-insensitive component = 8.4 ± 3.0% of initial response; n = 4 cells). Thus, gap junctions contribute substantially to light-driven signals in ON cone bipolar cells.

Coupling among bipolar cells is likely mediated primarily by gap junctions between ON cone bipolar cells and AII amacrine cells (Tsukamoto et al., 2001; Marc et al., 2014; Veruki and Hartveit, 2002a). However, the experiment in Figures 3B–3D cannot rule out additional contributions from direct coupling between bipolar cells (Arai et al., 2010; Cohen and Sterling, 1990) or coupling between bipolar cells and other amacrine cell types (Lee et al., 2015).

It is important to note that saturating flash responses in ON cone bipolar cells in *Cx36*$^{-/-}$ tissue were on average less than half as large as those from wild-type mice (peak amplitude = −20 ± 2 pA versus −46 ± 4 pA; n = 4 and 14 cells; Figure 3D). Furthermore, much stronger flashes were required to evoke saturating responses in *Cx36*$^{-/-}$ versus wild-type retinas (~600R*/rod/flash from darkness versus ~100R*/rod/flash from ~600R*/rod/s background). Smaller, less sensitive ON bipolar cell light responses should result in diminished excitatory synaptic transmission onto amacrine cells and RGCs, and this could have important consequences for retinal processing in *Cx36*$^{-/-}$ mice (see below). Multiple mechanisms could contribute to such effects given the expression of connexin36 at several locations in the retina (Deans et al., 2002).

## Gap Junctions Are Required for Supralinear Integration

We next examined whether electrical synapses were required for nonlinear paired bar interactions. First, we recorded from ON-S RGCs in tissue from *Cx36*$^{-/-}$mice. Unlike in wild-type tissue, responses in recordings from *Cx36*$^{-/-}$ retinas were linear or sublinear across all stimulus contrasts, from those that elicited just measurable responses (~10–20 pA) to contrasts that evoked maximal currents (Figures 3E–3H). The lack of supralinear responses in *Cx36*$^{-/-}$ mice is consistent with a role for gap junctions in mediating nonlinear interactions between bipolar cells. However, as expected from our bipolar cell recordings in these mice, higher stimulus contrasts were required to elicit responses in *Cx36*$^{-/-}$ retina (compare Figures 2 and 3E–3H) and peak excitatory currents in ON-S RGCs were ~60% as large in *Cx36*$^{-/-}$ cells (−503 ± 45 pA, n = 5) compared to wild-type cells (−786 ± 79 pA, n = 10). Thus, a disrupted retinal network state in *Cx36*$^{-/-}$ animals could contribute to the loss of supralinear paired bar interactions.

As an alternative test, we examined the effect of meclofenamic acid (MFA), which has been used to block gap-junction-mediated signaling in the retina (Veruki and Hartveit, 2009; Pan et al., 2007). Bath application of MFA (100 μM) abolished supralinear integration (NLI control = 0.59 ± 0.07; in MFA = 0.03 ± 0.13; n = 5; p = 0.007, paired t test), supporting our hypothesis that lateral paired bar interactions are mediated by gap junctions (Figures S3A and S3B). However, results from experiments using MFA should be interpreted cautiously because MFA application substantially affected retinal sensitivity and health, likely related to poor specificity of the drug (see Supplemental Experimental Procedures for in-depth discussion).

Additional mechanisms besides electrical coupling among bipolar cells could contribute to lateral interactions within the bipolar cell network. For example, amacrine-cell-mediated inhibition and/or activation of presynaptic glutamate transporters by glutamate spillover (Veruki et al., 2006) can influence bipolar cell synaptic output. Experiments in which we bath applied inhibitory receptor antagonists argue against a role for inhibitory mechanisms in establishing supralinear paired bar interactions (Figures S3C–S3F). Although we did not test for a role for glutamate transporters, we consider it unlikely that glutamate transporters expressed on bipolar cell axon terminals could contribute to supralinear paired bar integration because the chloride conductance associated with glutamate transport should hyperpolarize bipolar cell axons (Duebel et al., 2006; Veruki et al., 2006). Thus, paired bar stimuli, which should elicit more glutamate release than single bar stimuli, should exhibit sublinear rather than supralinear interactions if axonal glutamate transporters have an important influence.

Our findings that gap junctions contribute substantially to ON cone bipolar cell light responses (Figures 3A–3D), that inhibitory mechanisms do not contribute to supralinear paired bar responses (Figures S3C–S3F), and that supralinear integration is absent in MFA (Figures S3A and S3B) or in tissue from *Cx36*$^{-/-}$mice (Figures 3E–3H) together make a strong case for an important role for inner retina gap junctions in mediating lateral interactions.

## Cone Bipolar Synapses Are the Site of Nonlinear Integration

We next sought to identify the nonlinear mechanism(s) underlying paired bar interactions. As in most neurons, release of neurotransmitter from bipolar cell synapses is low at hyperpolarized presynaptic membrane potentials but increases sharply with depolarization (Burrone and Lagnado, 2000; Jarsky et al., 2011). Thus, the strong enhancement to paired positive contrast bars at low stimulus strength (Figure 2) could arise due to modulation of bipolar membrane potential near a transition between low and high synaptic output, where small changes in bipolar cell voltage should strongly influence neurotransmitter release. Similarly, hyperpolarizing responses to negative contrast stimuli could suppress bipolar output (Figure 1E) by moving bipolar

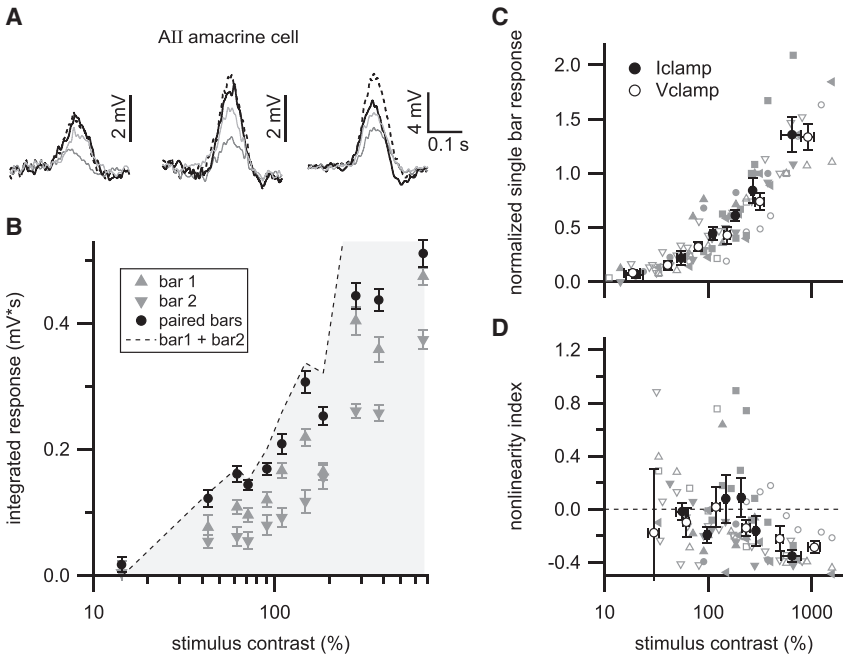


**Figure 4. Linear or Sublinear Responses in AII Amacrine Cells**

(A) Mean voltage responses at different stimulus contrasts in an example AII amacrine cell (flat mount retina). Resting membrane potential, −47 mV. Stimulus contrasts (left to right): 62%, 110%, and 281%.

(B) Contrast-response relationship for cell shown in (A). Symbols show mean ± SEM.

(C) Summary of AII amacrine cell responses across contrasts. Filled gray symbols (single cell) and filled black circles with error bars (mean ± SEM) show data from current-clamp recordings (n = 5 cells; resting membrane potential = −48 ± 2 mV). Open gray symbols (single cell) and white circles with error bars (mean ± SEM) are from voltage-clamp recordings (n = 4 cells).

(D) Summary of nonlinearity index versus stimulus contrast. Same symbol and color scheme as in (C).

cell synapses away from threshold for neurotransmitter release. Mechanisms upstream of bipolar cell synaptic transmission—for example, activation of voltage-dependent conductances in cone bipolar cells (Puthussery et al., 2013; Saszik and DeVries, 2012) or nonlinear synaptic transmission from cones to cone bipolar cells—could also contribute to nonlinear integration of paired bar stimuli.

We tested for contributions of mechanisms prior to bipolar cell synaptic output by recording from AII amacrine cells. Because AII amacrine cells are electrically coupled to ON cone bipolar cell axon terminals, their responses provide a measure of visually evoked signals in the ON cone bipolar circuitry prior to glutamate release from cone bipolar cell synapses (see Figure 1A). Thus, if nonlinear integration occurs at any location upstream of cone bipolar synaptic output, paired bar responses of AIIs should resemble those of RGCs. However, paired bar responses in AII amacrine cells, measured as excitatory input currents or as voltage responses, were linear across the range of contrasts that produced supralinear responses in ON-S RGCs (Figures 4A–4D). These results argue against substantial contributions to nonlinear paired bar interactions from potential upstream (e.g., nonlinearity of cone synapse or cone bipolar cell intrinsic response) or AII-intrinsic mechanisms (e.g., voltage-dependent conductances) (Tian et al., 2010).

These results constrain the mechanism of nonlinear integration to a process operating at ON cone bipolar synaptic terminals. We therefore consider it likely that glutamate release from ON cone bipolar terminals constitutes the principal nonlinear mechanism underlying nonlinear integration of signals across different bipolar cells.

## Bipolar Network Model Reproduces Nonlinear Effects

The results presented in Figures 1, 2, 3, and 4 support a mechanistic description of nonlinear integration in the bipolar cell network. Lateral signals, mediated by gap junctional coupling between AII amacrine cells and ON cone bipolar axon terminals, combine with feed-forward (cone→cone bipolar dendrite) signals to generate changes in bipolar cell membrane potential (Figure 3). As reflected in recordings from AII amacrine cells, this combination of feed-forward and lateral voltage signals in bipolar cells is linear (Figure 4), but the subsequent nonlinear transformation of bipolar cell membrane potential into release of glutamate results in nonlinear synaptic output. To further test this idea, we incorporated lateral interactions and nonlinear synaptic output into a model of the type 6 cone bipolar cell population.

A realistic spatial distribution of bipolar cells was constructed by forming a non-overlapping mosaic of bipolar cell axon territories drawn from anatomical measurements of type 6 axon terminals (Schwartz et al., 2012). For each bipolar cell, direct dendritic input from cones was modeled by weighting stimuli according to a circular 2D Gaussian profile with dimensions based on the dendritic morphology of type 6 bipolar cells (Figure 5A, top left) (Schwartz et al., 2012). Electrotonic spread of signals through gap junctions was implemented by spreading a fraction of direct dendritic input in a given bipolar cell to surrounding bipolar cells; the magnitude of this signal spread decayed exponentially with distance between bipolar cell center positions (Figure 5A, bottom left) (Lamb and Simon, 1976).

This model reproduced the previously determined receptive field profile of type 6 cone bipolar cells (Figure 5B) using reasonable, though not unique, values for the parameters controlling electrical signal spread (Figure 5A, bottom). Additionally, the fraction of bipolar cell response attributable to lateral input using these model parameters (46.5 ± 0.2%, n = 5 model bipolar populations, mean ± SEM) was close to that estimated by dialyzing bipolar cells with GTP-γ-S (35.8 ± 6.6% for n = 10 type 6 bipolar cells; 42.8 ± 4.1% for n = 18 bipolar cells across types).

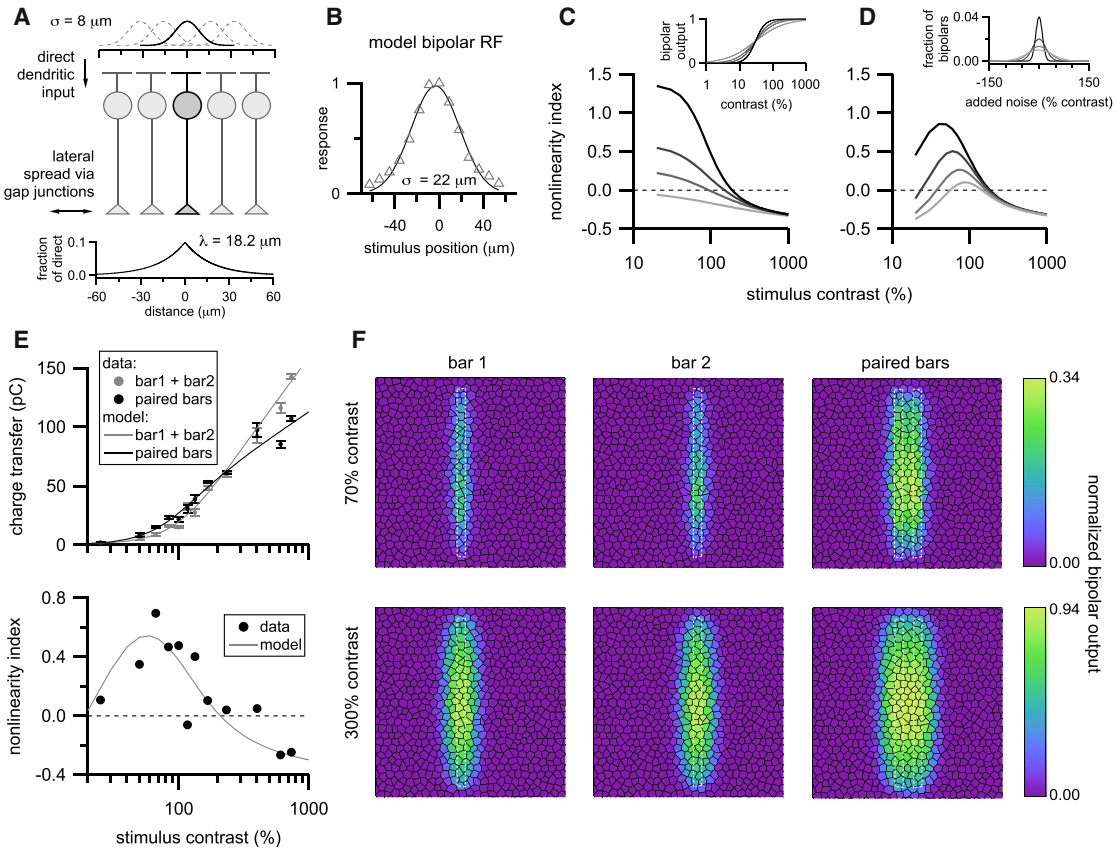


**Figure 5. Simplified Model of Synaptic Output from Bipolar Cell Population**

(A) Dendritic input to ON cone bipolar cells was modeled by filtering stimuli by a circular Gaussian profile matched to the anatomical dimensions of type 6 bipolar dendrites (top; σ = SD of Gaussian). Gap-junction-mediated signals were modeled by spreading a fraction of dendritic signals to neighboring bipolar locations according to an exponential function (bottom; λ = space constant).

(B) Example modeled spatial response profile (triangles) of a bipolar cell to narrow bars of light using parameters shown in (A). Solid curve is a Gaussian function fitted to the model responses. For five independently generated model populations, 2 SD diameter of Gaussian profile for model responses = 43.4 ± 0.4 μm (experimentally measured = 44 ± 8 μm) (Schwartz et al., 2012).

(C) Effect of nonlinear bipolar output. Gray lines of increasing darkness are modeled nonlinear interactions for paired bar stimuli for bipolar output nonlinearities with increasing steepness ($h$ = 1, 1.5, 2, 3; see inset). All other model parameters were kept constant. These curves show output from model without bipolar noise.

(D) Effect of adding noise. Gray lines of increasing darkness show nonlinear interactions for increasing amounts of additive noise ($\sigma_{bipolar}$ = 10%, 20%, 30%, and 40% contrast; see inset) upstream of a fixed synaptic nonlinearity ($x_{half}$ = 30% contrast, $h$ = 3).

(E) Comparison of bar responses (top) and associated nonlinearity indices across contrasts (bottom) from an example ON-S RGC (symbols; error bars in top panel show SEM) and output of the model (solid lines) ($c_{half}$ = 37%; $h$ = 2.52; $\sigma_{bipolar}$ = 14%).

(F) Representation of model output from individual bipolar cells (black hexagons) across the population for single (left, middle) and paired bars (right) at stimulus contrasts producing robust supralinear paired bar responses (70%, top row) or sublinear interactions (300%, bottom row). Note different color scales for top versus bottom panels. Each panel is a 400 μm by 400 μm region of the bipolar population and shows the average bipolar output across ten stimulus presentations with bipolar noise values generated by different random seeds. White dotted lines show boundaries of bar stimuli.

Synaptic output from each bipolar cell ($r$) was modeled by transforming the linear combination of dendritic and lateral signals ($c_{total}$) according to a sigmoidal Hill function that approximated the nonlinear relation between presynaptic voltage and synaptic output:

$$r_i = \frac{1}{1 + \left(\frac{c_{half}}{c_{total(i)}}\right)^h},$$

where $c_{half}$ and $h$ are parameters that determine the offset along the contrast axis and steepness of the contrast-response function. The output of each bipolar cell was then weighted and summed to simulate excitatory synaptic input to an ON-S RGC. For simplicity, bipolar weights were drawn from a Gaussian profile matching the receptive field size of ON-S RGCs.

Using this model, we explored how nonlinear synaptic output contributes to integration of paired bar stimuli. As shown in Figure 5C, when the relationship between bipolar cell response and synaptic output was made steeper, by increasing the exponent ($h$) in the Hill function, modeled paired bar responses became progressively more supralinear. Further, for approximately linear bipolar cell output ($h$ = 1), modeled responses were linear or sublinear across contrasts (Figure 5C, light gray line). These observations indicate a critical role for nonlinear bipolar synaptic

output in the supralinear integration of lateral and feed-forward bipolar signals.

An unrealistic assumption in the model as implemented in Figure 5C is that every bipolar cell in the model population starts from the same initial "resting" state prior to stimulus presentation. Because current flow across gap junctions is driven by intercellular voltage differences, heterogeneity in pre-stimulus resting membrane potential among bipolar cells should impact how electrical signals spread within the bipolar network. We therefore tested the effect of introducing variability into the modeled bipolar cell population by randomly assigning an initial contrast, drawn from a Gaussian distribution, to each bipolar cell (Figure 5D). Adding a small amount of variability into bipolar cells upstream of their synaptic nonlinearity primarily affected modeled responses at low stimulus contrasts and resulted in a better match to the experimentally observed decrease in nonlinear integration for low contrasts. Further, for a fixed bipolar cell synaptic nonlinearity, increasing variability in pre-stimulus bipolar resting state progressively suppressed nonlinear paired bar interactions. These effects were likely the combined result of changes in spread of gap-junction-mediated signals and the fact that increasing variability in the bipolar cell population progressively biased output synapses toward more linear regions of their input-output relationship.

When the parameters controlling nonlinearity of bipolar synaptic output ($c_{half}$ and $h$) and variability in initial bipolar resting state (SD of the Gaussian noise distribution, $\sigma_{bipolar}$) as well as an overall scale factor were adjusted to fit single and paired bar responses recorded from ON-S RGCs, the model was able to reproduce the nonlinear integration we measured experimentally in both individual cells (Figure 5E) and across cells (Figures 2C and 2D).

Examination of the model output from individual bipolar cells provides insight into why supralinear integration occurs preferentially at low stimulus contrast. As shown in the top panels of Figure 5F, simultaneous presentation of low contrast, closely spaced bars had two clear effects: (1) increased output from those bipolar cells receiving direct stimulation from either bar and (2) strongly increased output in response to paired bar stimuli from bipolar cells primarily receiving indirect, lateral input (those in between the bars). At higher stimulus contrast, output from some directly stimulated bipolar cells can be saturated by the single bar stimuli and indirectly stimulated bipolar cells are activated sufficiently by single bars to produce significant output (Figure 5D, bottom). Because of the high degree of overlap in the populations of depolarized bipolar cells for high contrast single bars, responses to paired bar stimuli are smaller than the sum of single bar responses.

The model of Figure 5 shows that nonlinear integration of paired-bar stimuli can be explained by a combination three factors: (1) lateral interactions through gap junctions, (2) variability in bipolar cell resting potential, and (3) a nonlinear relationship between bipolar cell voltage and synaptic output.

## Nonlinear Integration in Additional RGC Types

The experiments and modeling in Figures 1, 2, 3, 4, and 5 focused specifically upon ON-S RGCs. We examined responses in additional RGC types to further test the idea that an interaction between gap-junction-mediated lateral interactions and nonlinear synaptic output contributes to supralinear integration of paired bar stimuli.

We first measured synaptic currents in OFF sustained (OFF-S) RGCs, which receive glutamatergic input from OFF bipolar cells and glycinergic input from ON bipolar cell-driven amacrine cells, including AII amacrine cells (Murphy and Rieke, 2006, 2011; van Wyk et al., 2009). In OFF-S RGCs, negative contrast paired bar stimuli elicited excitatory synaptic currents that were equal to or less than the sum of single bar responses (Figures S4B–S4D, left). This lack of supralinear integration is probably because, unlike ON bipolar cells, OFF bipolar cells are not extensively electrically coupled with each other. Unlike excitatory input, inhibitory synaptic currents in OFF-S RGCs elicited by positive contrast paired bars were moderately supralinear over the same range of contrasts that evoked supralinear paired bar responses in ON-S RGCs (Figures S4B–S4D, right). This could be the result of gap-junction-mediated lateral signal spread among AII amacrine cells prior to nonlinear glycine release from AII amacrine cell axons and/or inheritance of nonlinear responses from ON cone bipolar cells by additional ON amacrine cells providing input to OFF-S RGCs.

ON-S RGCs receive excitatory input primarily from type 6 cone bipolar cells (Schwartz et al., 2012), but all or nearly all ON cone bipolar types form electrical synapses with AII amacrine cells (Cohen and Sterling, 1990; Marc et al., 2014; Veruki and Hartveit, 2002a). Indeed, we observed GTP-γ-S-insensitive light responses in all ON cone bipolar types tested (Figure 3D). We therefore examined responses to single and paired bar stimuli in a different ON RGC type, which we term ON transient (ON-T) based on its characteristic response to light steps (Figure S4A). ON-T cells receive excitatory synaptic input primarily from type 5 bipolar cells (S.P. Kuo, H. Okawa, R. Wong and F. Rieke, unpublished data). Similar to our results from ON-S RGCs, paired bar stimuli elicited supralinear excitatory synaptic currents in ON-T RGCs at low to moderate stimulus contrasts (Figures S4E–S4G). Taken together with our data from ON-S and OFF-S RGCs, these results suggest gap-junction-mediated lateral interactions among ON cone bipolar cells play an important role in how visual stimuli are integrated by multiple ON pathway circuits in the retina.

## Nonlinear Integration Enhances Responses to Stimuli with Spatiotemporal Correlations

How does the nonlinear integration revealed by paired bar stimuli shape RGC responses to more complex stimuli? The answer to this question depends critically upon the temporal and spatial scale over which nonlinear integration occurs.

We characterized the spatial scale of nonlinear integration by recording RGC responses to single or paired bars at different inter-bar spacings (Figures 6A and 6B). Paired bars were presented simultaneously and stimulus contrast was fixed for each cell at a value that elicited supralinear integration for small inter-bar spacing. Nonlinear integration occurred for bar spacings up to 60–80 μm (Figure 6B; space constant of exponential fit to spacing >36 μm = 21 μm); this is somewhat larger than the receptive field diameter of type 6 bipolar cells (~44 μm;

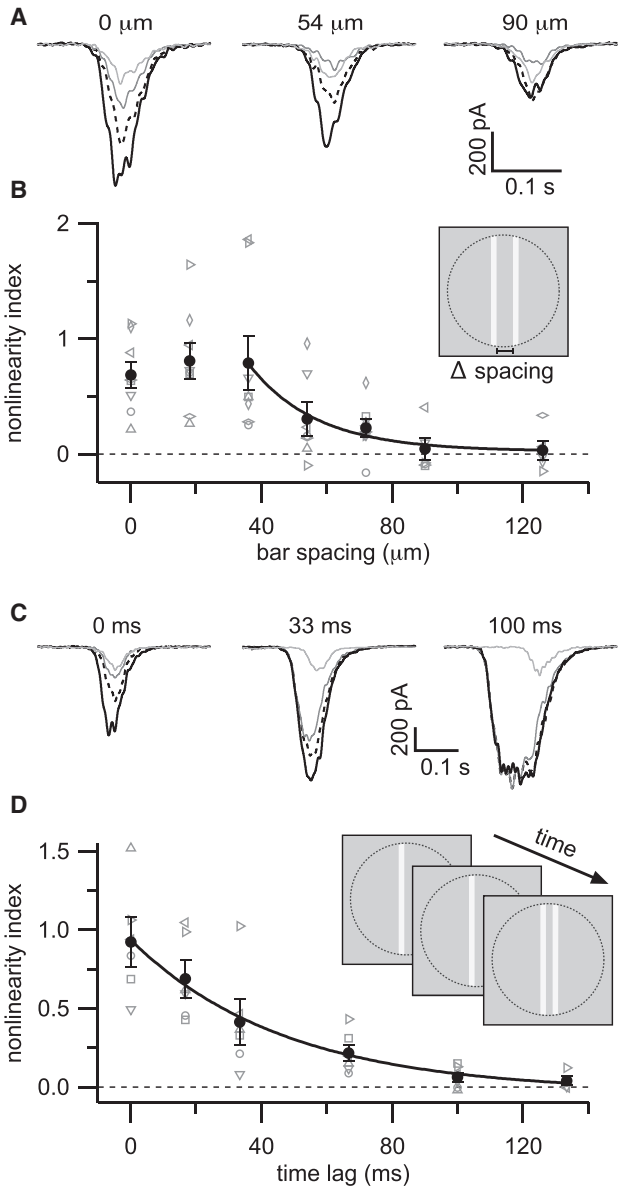


**Figure 6. Nonlinear Interactions Extend over Space and Time**

(A) Mean responses from an example ON-S RGC to stimuli presented at different inter-bar spacings.

(B) Summary of nonlinearity index versus inter-bar spacing. Gray symbols are data from individual cells. Black circles show mean ± SEM (n = 8 cells). Solid black line shows exponential fit (λ = 21 μm) to points between 36 and 126 μm. Paired bars were presented simultaneously (33 ms flash). Stimulus contrasts were held constant across locations for each cell.

(C) Mean responses from an example ON-S RGC to stimuli presented with different time lags between first and second bar presentations.

(D) Summary of nonlinearity index versus inter-bar time differences. Gray symbols are data from individual cells. Black circles show mean ± SEM (n = 6 cells). Black line shows exponential fit to data (τ = 47 ms). Stimulus contrast and positions were held constant across time lags (inter-bar distance 22 μm). Line style in (A) and (C) follows that used in Figure 2.

Schwartz et al., 2012) and several times larger than the anatomical dimensions of type 6 bipolar dendrites (~15–17 μm diameter; Bleckert et al., 2014; Dunn and Wong, 2012; Wässle et al., 2009). Thus, signals can spread across multiple nearby bipolar cells to interact nonlinearly.

We tested the temporal scale of nonlinear integration in a separate set of experiments in which one bar was presented and kept on for varying amounts of time before flashing a second bar. The spatial relationship between bars and the stimulus contrasts were kept fixed across the time delays tested. The first bar was kept on until the flashed second bar disappeared to avoid complications arising from offset responses to brief flash stimuli. Nonlinear integration was strongest for simultaneously presented stimuli, but also occurred for stimuli with short temporal delays between bar presentations (Figures 6C and 6D). The decrease in nonlinearity index with increasing time between bar presentations was well-fit by an exponential function with a time constant of 47 ms from the onset of the first bar (Figure 6D), which is shorter than the flash response duration in ON-S RGCs (~100 ms).

The spatially and temporally restricted extent of nonlinear integration revealed in these experiments suggests that for low stimulus contrasts, ON-S RGCs should respond preferentially to stimuli with strong spatiotemporal correlations. We tested this prediction by comparing ON-S RGC responses to two stimuli that differed in the strength of their spatiotemporal correlations: (1) an apparent motion stimulus, in which a narrow (width = 18 μm), positive contrast bar moved incrementally across the receptive field of a recorded RGC on successive frames of the stimulus presentation (Figure 7A, left; "sequential"), and (2) a stimulus that was identical in all respects except the order of stimulus frame presentations was randomized in each trial (Figure 7A, right; "randomized").

The total stimulus duration and cumulative bar positions were the same in both stimuli, and hence linear integration should result in identical average responses when integrated over the stimulus presentation time. However, ON-S RGC excitatory synaptic inputs and spike outputs were greater to the apparent motion stimulus at low to moderate stimulus contrasts (Figures 7B–7E). The similarity of spike output and excitatory input in these experiments is consistent with previous work demonstrating ON-S RGC spike output is dominated by excitation at the background light level used here (Schwartz et al., 2012). Notably, the relationship between stimulus contrast and sensitivity to the apparent motion versus the randomized stimulus (Figure 7E) was similar to that for nonlinear integration of paired bar stimuli (Figure 2D).

We observed enhanced ON-S RGC sensitivity to the sequential versus randomized bar stimulus across a range of apparent motion speeds (0.2 to 1.1 mm/s [the upper limit of our stimulus monitor]) (Figure S6). This finding is consistent with the spatial extent of supralinear paired bar integration characterized in Figures 6A and 6B, which predicts that enhanced sensitivity should occur for bar motion speeds up to ~1.7 mm/s (corresponding to a 57 μm bar movement within the 33 ms flash duration of the stimuli used in Figures 7A and 7B). Thus, nonlinear integration within the bipolar network enhances RGC sensitivity to stimuli with strong spatiotemporal correlations.

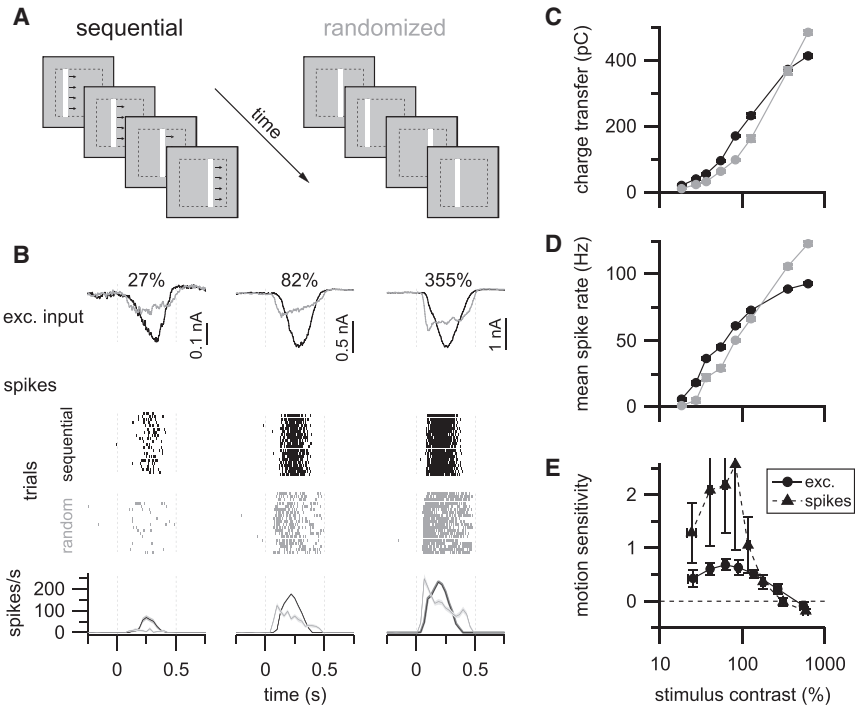


**Figure 7. ON-S RGCs Exhibit Enhanced Sensitivity to Spatio-Temporally Correlated Stimuli**

(A) Stimulus paradigm for comparing spatiotemporally correlated ("sequential," left) or uncorrelated ("randomized," right) stimuli.

(B) Mean excitatory current (top row; whole-cell) and spike (bottom rows; cell-attached) responses from the same example ON-S RGC at different bar contrasts. Raster plots in middle rows show spike responses to twenty presentations of each stimulus type. Here, "sequential" and "randomized" trials are separated for visual clarity, but stimulus trials were interleaved in the experiment. Lines and light shaded regions in peristimulus time histograms in bottom row show mean ± SEM spike rate, bin width = 30 ms.

(C and D) Summary responses across contrasts for excitatory input (C) and spikes (D) for same cell as shown in (B). Averaged responses in (B)–(D) are from 25 trials of each stimulus type.

(E) Summary of sequential versus randomized stimulus response as function of stimulus contrast for excitatory currents (filled circles, n = 5 cells) and spikes (open circles, n = 6 cells). Symbols and error bars in (C)–(E) are mean ± SEM (error bars mostly obscured by symbols in [C] and [D]). Bar speed = 0.86 mm/s (stimulus duration = 0.416 s). See also Figure S6.

## DISCUSSION

We found that electrical coupling strongly influences how the retinal ON cone bipolar network integrates visual stimuli. By influencing neurotransmitter release from bipolar cell axons, lateral spread of signals among neighboring bipolar cells can selectively enhance bipolar synaptic output in response to low-contrast stimuli that occur closely in space and time. Recent work demonstrates an important role for electrical coupling in postsynaptic integration of combined electrical and chemical synaptic inputs (Trenholm et al., 2013b, 2014; Vervaeke et al., 2012), and in controlling steady-state release properties of chemical synapses (Grimes et al., 2014); our results complement these findings to highlight how electrical and chemical synapses can work in concert to dictate circuit function.

### Roles for AII Amacrine Cells beyond Rod-Mediated Vision

AII amacrine cells have a central role in vision under dim light (scotopic) conditions (Bloomfield and Dacheux, 2001). Our results are consistent with and extend previous studies demonstrating an important role for gap junctions between ON cone bipolar cells and AII amacrine cells in shaping signaling under conditions where cones contribute to visual processing (Liang and Freed, 2010; Manookin et al., 2008; Münch et al., 2009; reviewed in Demb and Singer, 2012).

In principle, spatial spread of signals could occur in the outer retina and/or in the inner retina. Several findings implicate a dominant role of AII amacrine-ON cone bipolar gap junctions in the nonlinear integration we studied here. First, the prominent gap-junction-mediated component of light responses in ON cone bipolar cells (Figure 3) was insensitive to suppression of dendritic input to the recorded bipolar cell, and hence must originate through effective coupling between bipolar cells. This is consistent with previous measurements of robust AII-AII and AII-ON cone bipolar coupling (Trexler et al., 2005; Veruki and Hartveit, 2002a, 2002b). Second, anatomical evidence suggests extensive coupling among AII amacrine cells and between AII amacrine cells and ON cone bipolar terminals (Tsukamoto et al., 2001; Tsukamoto and Omi, 2013), but electrical coupling in mouse outer retina appears primarily restricted to local syncytia of neighboring rods and overlapping rods and cones (Tsukamoto et al., 2001). Considering these anatomical differences between electrical networks in mouse inner and outer retina, the spatial scale of nonlinear integration (Figures 6A and 6B) seems more consistent with a prominent role for inner retinal coupling. Finally, our model of the bipolar cell network, which only incorporated coupling among bipolar cells, was able to recapitulate the nonlinear paired bar effects we measured experimentally.

Thus, extensive electrical coupling among AII amacrine cells and cone bipolar cells, together with nonlinear synaptic output from cone bipolar cells, endows the ON cone bipolar network with enhanced sensitivity to stimuli with spatiotemporal correlations. This mechanism is distinct from those previously identified for direction-selective visual computations (reviewed in Borst and Euler, 2011). Unlike direction selective RGCs, ON-S RGCs do not exhibit a preference for specific directions of visual motion (data not shown; Estevez et al., 2012). However, the enhanced sensitivity to moving stimuli we uncovered here could be relevant to encoding of motion direction in populations of ON-S RGCs (Chichilnisky and Kalmar, 2003). Notably, numerous types of RGCs exhibit higher sensitivity to moving versus static stimuli (Marre et al., 2012).

Our recordings from ON-S, OFF-S, and ON-T RGCs provide evidence that nonlinear integration may be a general property of ON cone bipolar cell circuits. It will be important to examine whether potential differences in electrical coupling (Cohen and Sterling, 1990) or synaptic nonlinearities (Asari and Meister, 2012) impact the integrative properties of networks of ON cone bipolar cells providing input to distinct postsynaptic targets. Within this context, it is interesting to note we observed stronger supralinear paired bar responses for excitatory inputs to ON-T versus ON-S RGCs (peak NLI = 1.25 ± 0.17 (n = 5) versus 0.79 ± 0.07 (n = 19), respectively; p = 0.01, t test), and this difference in nonlinear integration was correlated with apparent differences in synaptic transmission between the populations of bipolar cells providing presynaptic input to these RGCs. Specifically, spontaneous glutamatergic input appeared to be lower in ON-T compared to ON-S RGCs (Figures S5A and S5B) and excitatory input to ON-T RGCs had a steeper contrast-response relationship (Figures S5C and S5D). These observations suggest synaptic transmission from presynaptic bipolar cells to ON-T RGCs is more strongly nonlinear than transmission to ON-S RGCs, which could contribute to enhanced paired bar responses in ON-T RGCs.

In both ON RGC types, supralinear integration was restricted to stimulus contrasts below ~200%. This is likely because the relationship between bipolar cell membrane potential and glutamate release transitions sharply from a shallow to a steep slope over a narrow voltage range near resting membrane potential that corresponds to the activation threshold for presynaptic calcium channels (Burrone and Lagnado, 2000; Jarsky et al., 2010, 2011); at voltages beyond this threshold, there is an approximately linear transformation of membrane potential into synaptic output due to the nearly linear relationship between presynaptic calcium current and exocytosis once calcium channel open probability is high (Jarsky et al., 2010).

### Context-Dependent Signaling in Gap Junctional Networks

Recent work has highlighted how the functional properties of RGCs can change dramatically across different stimulus conditions (Geffen et al., 2007; Grimes et al., 2014; Rivlin-Etzion et al., 2012; Tikidji-Hamburyan et al., 2015). Such flexibility enhances the computational capacity of retinal circuits and presumably tunes retinal function to the specific demands of different visual environments (Grimes et al., 2014). Of relevance to our work, changes in background light levels can affect both electrical coupling among AII amacrine cells (Bloomfield et al., 1997) as well as the degree of bipolar cell synaptic nonlinearity (Grimes et al., 2014). Interestingly, we observed that supralinear integration of closely spaced bars was absent at ~100 R*/rod/s (Figure S2) but robust at higher light levels (~250 and 1,500R*/rod/s) (Figures 2 and S2). The mechanisms and functions of this transition in nonlinear integration within the mesopic range of visual processing is an interesting topic for future work.

### Stimulus-Selectivity from Gap Junctional Connectivity

Previous studies have established well-defined roles for gap junctions in enhancing signal to noise ratio (DeVries et al., 2002; Lamb and Simon, 1976; Smith and Vardi, 1995) or generating coordinated activity across electrically coupled networks (reviewed in Bennett and Zukin, 2004). Our findings show how gap junctions can impact circuit function by influencing synaptic output beyond simply synchronizing the release of neurotransmitter across populations of cells (Beierlein et al., 2000). Our results may have general relevance to other electrically coupled networks. Although we studied bipolar cells, which are non-spiking neurons with specialized ribbon-type synapses, subthreshold changes in presynaptic membrane potential can also control neurotransmitter release from spiking neurons (Alle and Geiger, 2006; Awatramani et al., 2005; Shu et al., 2006). Thus, interaction between electrical coupling and nonlinear chemical synaptic transmission may endow the postsynaptic targets of diverse electrically coupled networks with preferential sensitivity to those patterns of afferent input that simultaneously or near-simultaneously engage lateral and feed-forward signals.

## EXPERIMENTAL PROCEDURES

Experimental procedures are summarized briefly below. See Supplemental Experimental Procedures for additional description as well as details of the modeling.

### Electrophysiology

Experiments were conducted in tissue obtained from dark-adapted 5- to 15-week-old mice. Animal care and handling followed procedures approved by the Institutional Animal Care and Use Committee of the University of Washington. RGC and AII amacrine recordings were conducted in a flat-mount preparation. Bipolar cell recordings were obtained from a retinal slice preparation. During recordings, tissue was continuously perfused (~8 mL/min) with oxygenated (95% $O_2$, 5% $CO_2$), bicarbonate-buffered Ames solution maintained at 30°C–34°C. Whole-cell voltage-clamp recordings were obtained using patch pipettes filled with a $Cs^+$-based internal solution. For bipolar cell recordings, this internal solution also included 50–100 μM GTP-γ-S and 100–200 μM Alexa Fluor 594 and 10 μM NBQX (Tocris) was added to the bath perfusion solution. Current-clamp recordings from AII amacrine cells used a $K^+$-based internal solution. RGC spiking activity was measured using loose-cell attached recordings.

### Visual Stimulation

Stimuli from an OLED monitor (eMagin; 800 × 600 pixels, 1.2 or 1.8 μm per pixel at the preparation; 60 Hz frame rate; RGC and AII recordings) or short wavelength LED (520 μm diameter uniform spot, peak spectral output 405 nm; Hosfelt; bipolar cell recordings) were projected through the microscope condenser and focused on the photoreceptor layer. Stimulus contrast ($c$) was defined as

$$c = \left(\frac{I - b}{b}\right) \times 100\%,$$

where $I$ = stimulus intensity and $b$ = background light intensity. RGC and AII amacrine recordings were performed with a background light intensity of ~250 rhodopsin isomerizations per rod per second (R*/rod/s) except in Figure S2 (calculated from the stimulus power and spectral output, rod spectral sensitivity, and an assumed rod collecting area of 0.5 $\mu m^2$) (Field and Rieke, 2002). Bipolar cell responses were measured on a background of ~600 R*/rod/s except for recordings from $Cx36^{-/-}$ tissue, when responses were obtained from nominal darkness due to reduced sensitivity of bipolar cells in $Cx36^{-/-}$ retinas.

## SUPPLEMENTAL INFORMATION

Supplemental Information includes six figures and Supplemental Experimental Procedures and can be found with this article online at http://dx.doi.org/10.1016/j.neuron.2016.03.012.

## AUTHOR CONTRIBUTIONS

S.P.K., G.W.S., and F.R. designed experiments. S.P.K. acquired and analyzed data. G.W.S. and S.P.K. performed modeling. S.P.K. and F.R. wrote manuscript.

## ACKNOWLEDGMENTS

We thank Gautam Awatramani, Will Grimes, Gabe Murphy, and Max Turner for suggestions on an earlier version of the manuscript; Mike Ahlquist, Mark Cafaro, Shellee Cunnington, and Paul Newman for outstanding technical support; Josh Singer for providing *Gjd2-EGFP* mice and Rachel Wong for providing *Gus8.4-EGFP* mice; and members of the Rieke lab for helpful feedback throughout this project. This work was supported by NIH (EY11850 to F.R.) and the Howard Hughes Medical Institute (F.R.).

Received: August 2, 2015
Revised: February 2, 2016
Accepted: March 6, 2016
Published: April 7, 2016

## REFERENCES

Alle, H., and Geiger, J.R. (2006). Combined analog and action potential coding in hippocampal mossy fibers. Science *311*, 1290–1293.

Arai, I., Tanaka, M., and Tachibana, M. (2010). Active roles of electrically coupled bipolar cell network in the adult retina. J. Neurosci. *30*, 9260–9270.

Asari, H., and Meister, M. (2012). Divergence of visual channels in the inner retina. Nat. Neurosci. *15*, 1581–1589.

Asteriti, S., Gargini, C., and Cangiano, L. (2014). Mouse rods signal through gap junctions with cones. eLife *3*, e01386.

Attwell, D., and Wilson, M. (1980). Behaviour of the rod network in the tiger salamander retina mediated by membrane properties of individual rods. J. Physiol. *309*, 287–315.

Awatramani, G.B., Price, G.D., and Trussell, L.O. (2005). Modulation of transmitter release by presynaptic resting potential and background calcium levels. Neuron *48*, 109–121.

Baccus, S.A., Olveczky, B.P., Manu, M., and Meister, M. (2008). A retinal circuit that computes object motion. J. Neurosci. *28*, 6807–6817.

Beierlein, M., Gibson, J.R., and Connors, B.W. (2000). A network of electrically coupled interneurons drives synchronized inhibition in neocortex. Nat. Neurosci. *3*, 904–910.

Bennett, M.V., and Zukin, R.S. (2004). Electrical coupling and neuronal synchronization in the Mammalian brain. Neuron *41*, 495–511.

Berntson, A., and Taylor, W.R. (2000). Response characteristics and receptive field widths of on-bipolar cells in the mouse retina. J. Physiol. *524*, 879–889.

Bleckert, A., Schwartz, G.W., Turner, M.H., Rieke, F., and Wong, R.O. (2014). Visual space is represented by nonmatching topographies of distinct mouse retinal ganglion cell types. Curr. Biol. *24*, 310–315.

Bloomfield, S.A., and Dacheux, R.F. (2001). Rod vision: pathways and processing in the mammalian retina. Prog. Retin. Eye Res. *20*, 351–384.

Bloomfield, S.A., Xin, D., and Osborne, T. (1997). Light-induced modulation of coupling between AII amacrine cells in the rabbit retina. Vis. Neurosci. *14*, 565–576.

Borst, A., and Euler, T. (2011). Seeing things in motion: models, circuits, and mechanisms. Neuron *71*, 974–994.

Burrone, J., and Lagnado, L. (2000). Synaptic depression and the kinetics of exocytosis in retinal bipolar cells. J. Neurosci. *20*, 568–578.

Chang, L., and He, S. (2014). Light adaptation increases response latency of alpha ganglion cells via a threshold-like nonlinearity. Neuroscience *256*, 101–116.

Chichilnisky, E.J., and Kalmar, R.S. (2003). Temporal resolution of ensemble visual motion signals in primate retina. J. Neurosci. *23*, 6681–6689.

Christie, J.M., and Westbrook, G.L. (2006). Lateral excitation within the olfactory bulb. J. Neurosci. *26*, 2269–2277.

Cohen, E., and Sterling, P. (1990). Demonstration of cell types among cone bipolar neurons of cat retina. Philos. Trans. R. Soc. Lond. B Biol. Sci. *330*, 305–321.

Dacey, D., Packer, O.S., Diller, L., Brainard, D., Peterson, B., and Lee, B. (2000). Center surround receptive field structure of cone bipolar cells in primate retina. Vision Res. *40*, 1801–1811.

Deans, M.R., Volgyi, B., Goodenough, D.A., Bloomfield, S.A., and Paul, D.L. (2002). Connexin36 is essential for transmission of rod-mediated visual signals in the mammalian retina. Neuron *36*, 703–712.

Demb, J.B., and Singer, J.H. (2012). Intrinsic properties and functional circuitry of the AII amacrine cell. Vis. Neurosci. *29*, 51–60.

Demb, J.B., Zaghloul, K., Haarsma, L., and Sterling, P. (2001). Bipolar cells contribute to nonlinear spatial summation in the brisk-transient (Y) ganglion cell in mammalian retina. J. Neurosci. *21*, 7447–7454.

Detwiler, P.B., and Hodgkin, A.L. (1979). Electrical coupling between cones in turtle retina. J. Physiol. *291*, 75–100.

DeVries, S.H., Qi, X., Smith, R., Makous, W., and Sterling, P. (2002). Electrical coupling between mammalian cones. Curr. Biol. *12*, 1900–1907.

Duebel, J., Haverkamp, S., Schleich, W., Feng, G., Augustine, G.J., Kuner, T., and Euler, T. (2006). Two-photon imaging reveals somatodendritic chloride gradient in retinal ON-type bipolar cells expressing the biosensor Clomeleon. Neuron *49*, 81–94.

Dunn, F.A., and Wong, R.O. (2012). Diverse strategies engaged in establishing stereotypic wiring patterns among neurons sharing a common input at the visual system's first synapse. J. Neurosci. *32*, 10306–10317.

Estevez, M.E., Fogerson, P.M., Ilardi, M.C., Borghuis, B.G., Chan, E., Weng, S., Auferkorte, O.N., Demb, J.B., and Berson, D.M. (2012). Form and function of the M4 cell, an intrinsically photosensitive retinal ganglion cell type contributing to geniculocortical vision. J. Neurosci. *32*, 13608–13620.

Farrow, K., Teixeira, M., Szikra, T., Viney, T.J., Balint, K., Yonehara, K., and Roska, B. (2013). Ambient illumination toggles a neuronal circuit switch in the retina and visual perception at cone threshold. Neuron *78*, 325–338.

Field, G.D., and Rieke, F. (2002). Nonlinear signal transfer from mouse rods to bipolar cells and implications for visual sensitivity. Neuron *34*, 773–785.

Freed, M.A., and Sterling, P. (1988). The ON-alpha ganglion cell of the cat retina and its presynaptic cell types. J. Neurosci. *8*, 2303–2320.

Galarreta, M., and Hestrin, S. (2001). Electrical synapses between GABA-releasing interneurons. Nat. Rev. Neurosci. *2*, 425–433.

Geffen, M.N., de Vries, S.E., and Meister, M. (2007). Retinal ganglion cells can rapidly change polarity from Off to On. PLoS Biol. *5*, e65.

Gollisch, T., and Meister, M. (2010). Eye smarter than scientists believed: neural computations in circuits of the retina. Neuron *65*, 150–164.

Grimes, W.N., Schwartz, G.W., Rieke, F., and Rieke, F. (2014). The synaptic and circuit mechanisms underlying a change in spatial encoding in the retina. Neuron *82*, 460–473.

Grimes, W.N., Graves, L.R., Summers, M.T., and Rieke, F. (2015). A simple retinal mechanism contributes to perceptual interactions between rod- and cone-mediated responses in primates. Elife *4*, http://dx.doi.org/10.7554/eLife.08033.

Helmstaedter, M., Briggman, K.L., Turaga, S.C., Jain, V., Seung, H.S., and Denk, W. (2013). Connectomic reconstruction of the inner plexiform layer in the mouse retina. Nature *500*, 168–174.

Jarsky, T., Tian, M., and Singer, J.H. (2010). Nanodomain control of exocytosis is responsible for the signaling capability of a retinal ribbon synapse. J. Neurosci. *30*, 11885–11895.

Jarsky, T., Cembrowski, M., Logan, S.M., Kath, W.L., Riecke, H., Demb, J.B., and Singer, J.H. (2011). A synaptic mechanism for retinal adaptation to luminance and contrast. J. Neurosci. *31*, 11003–11015.

Katz, B., and Miledi, R. (1967). A study of synaptic transmission in the absence of nerve impulses. J. Physiol. *192*, 407–436.

Lamb, T.D., and Simon, E.J. (1976). The relation between intercellular coupling and electrical noise in turtle photoreceptors. J. Physiol. *263*, 257–286.

Lee, S.C., Meyer, A., Schubert, T., Hüser, L., Dedek, K., and Haverkamp, S. (2015). Morphology and connectivity of the small bistratified A8 amacrine cell in the mouse retina. J. Comp. Neurol. *523*, 1529–1547.

Liang, Z., and Freed, M.A. (2010). The ON pathway rectifies the OFF pathway of the mammalian retina. J. Neurosci. *30*, 5533–5543.

Manookin, M.B., Beaudoin, D.L., Ernst, Z.R., Flagel, L.J., and Demb, J.B. (2008). Disinhibition combines with excitation to extend the operating range of the OFF visual pathway in daylight. J. Neurosci. *28*, 4136–4150.

Marc, R.E., Anderson, J.R., Jones, B.W., Sigulinsky, C.L., and Lauritzen, J.S. (2014). The AII amacrine cell connectome: a dense network hub. Front. Neural Circuits *8*, 104.

Marre, O., Amodei, D., Deshmukh, N., Sadeghi, K., Soo, F., Holy, T.E., and Berry, M.J., 2nd (2012). Mapping a complete neural population in the retina. J. Neurosci. *32*, 14859–14873.

Münch, T.A., da Silveira, R.A., Siegert, S., Viney, T.J., Awatramani, G.B., and Roska, B. (2009). Approach sensitivity in the retina processed by a multifunctional neural circuit. Nat. Neurosci. *12*, 1308–1316.

Murphy, G.J., and Rieke, F. (2006). Network variability limits stimulus-evoked spike timing precision in retinal ganglion cells. Neuron *52*, 511–524.

Murphy, G.J., and Rieke, F. (2011). Electrical synaptic input to ganglion cells underlies differences in the output and absolute sensitivity of parallel retinal circuits. J. Neurosci. *31*, 12218–12228.

Nakajima, Y., Iwakabe, H., Akazawa, C., Nawa, H., Shigemoto, R., Mizuno, N., and Nakanishi, S. (1993). Characterization of a novel retinal metabotropic glutamate receptor mGluR6 with a high agonist selectivity for L-2-amino-4-Phosphonobutyrate. J. Biol. Chem. *268*, 11868–11873.

Nawy, S., and Jahr, C.E. (1990). Suppression by glutamate of cGMP-activated conductance in retinal bipolar cells. Nature *346*, 269–271.

Pan, F., Mills, S.L., and Massey, S.C. (2007). Screening of gap junction antagonists on dye coupling in the rabbit retina. Vis. Neurosci. *24*, 609–618.

Pereda, A.E. (2014). Electrical synapses and their functional interactions with chemical synapses. Nat. Rev. Neurosci. *15*, 250–263.

Puthussery, T., Venkataramani, S., Gayet-Primo, J., Smith, R.G., and Taylor, W.R. (2013). NaV1.1 channels in axon initial segments of bipolar cells augment input to magnocellular visual pathways in the primate retina. J. Neurosci. *33*, 16045–16059.

Rivlin-Etzion, M., Wei, W., and Feller, M.B. (2012). Visual stimulation reverses the directional preference of direction-selective retinal ganglion cells. Neuron *76*, 518–525.

Sampath, A.P., and Rieke, F. (2004). Selective transmission of single photon responses by saturation at the rod-to-rod bipolar synapse. Neuron *41*, 431–443.

Saszik, S., and DeVries, S.H. (2012). A mammalian retinal bipolar cell uses both graded changes in membrane voltage and all-or-nothing Na+ spikes to encode light. J. Neurosci. *32*, 297–307.

Schwartz, E.A. (1976). Electrical properties of the rod syncytium in the retina of the turtle. J. Physiol. *257*, 379–406.

Schwartz, G., and Rieke, F. (2011). Perspectives on: information and coding in mammalian sensory physiology: nonlinear spatial encoding by retinal ganglion cells: when $1 + 1 \neq 2$. J. Gen. Physiol. *138*, 283–290.

Schwartz, G.W., Okawa, H., Dunn, F.A., Morgan, J.L., Kerschensteiner, D., Wong, R.O., and Rieke, F. (2012). The spatial structure of a nonlinear receptive field. Nat. Neurosci. *15*, 1572–1580.

Shiells, R.A., and Falk, G. (1990). Glutamate receptors of rod bipolar cells are linked to a cyclic GMP cascade via a G-protein. Proc. Biol. Sci. *242*, 91–94.

Shu, Y., Hasenstaub, A., Duque, A., Yu, Y., and McCormick, D.A. (2006). Modulation of intracortical synaptic potentials by presynaptic somatic membrane potential. Nature *441*, 761–765.

Slaughter, M.M., and Miller, R.F. (1981). 2-amino-4-phosphonobutyric acid: a new pharmacological tool for retina research. Science *211*, 182–185.

Smith, R.G., and Vardi, N. (1995). Simulation of the AII amacrine cell of mammalian retina: functional consequences of electrical coupling and regenerative membrane properties. Vis. Neurosci. *12*, 851–860.

Tian, M., Jarsky, T., Murphy, G.J., Rieke, F., and Singer, J.H. (2010). Voltage-gated Na channels in AII amacrine cells accelerate scotopic light responses mediated by the rod bipolar cell pathway. J. Neurosci. *30*, 4650–4659.

Tikidji-Hamburyan, A., Reinhard, K., Seitter, H., Hovhannisyan, A., Procyk, C.A., Allen, A.E., Schenk, M., Lucas, R.J., and Münch, T.A. (2015). Retinal output changes qualitatively with every change in ambient illuminance. Nat. Neurosci. *18*, 66–74.

Trenholm, S., McLaughlin, A.J., Schwab, D.J., and Awatramani, G.B. (2013a). Dynamic tuning of electrical and chemical synaptic transmission in a network of motion coding retinal neurons. J. Neurosci. *33*, 14927–14938.

Trenholm, S., Schwab, D.J., Balasubramanian, V., and Awatramani, G.B. (2013b). Lag normalization in an electrically coupled neural network. Nat. Neurosci. *16*, 154–156.

Trenholm, S., McLaughlin, A.J., Schwab, D.J., Turner, M.H., Smith, R.G., Rieke, F., and Awatramani, G.B. (2014). Nonlinear dendritic integration of electrical and chemical synaptic inputs drives fine-scale correlations. Nat. Neurosci. *17*, 1759–1766.

Trexler, E.B., Li, W., and Massey, S.C. (2005). Simultaneous contribution of two rod pathways to AII amacrine and cone bipolar cell light responses. J. Neurophysiol. *93*, 1476–1485.

Tsukamoto, Y., and Omi, N. (2013). Functional allocation of synaptic contacts in microcircuits from rods via rod bipolar to AII amacrine cells in the mouse retina. J. Comp. Neurol. *521*, 3541–3555.

Tsukamoto, Y., Morigiwa, K., Ueda, M., and Sterling, P. (2001). Microcircuits for night vision in mouse retina. J. Neurosci. *21*, 8616–8623.

van Wyk, M., Wässle, H., and Taylor, W.R. (2009). Receptive field properties of ON- and OFF-ganglion cells in the mouse retina. Vis. Neurosci. *26*, 297–308.

Veruki, M.L., and Hartveit, E. (2002a). Electrical synapses mediate signal transmission in the rod pathway of the mammalian retina. J. Neurosci. *22*, 10558–10566.

Veruki, M.L., and Hartveit, E. (2002b). AII (Rod) amacrine cells form a network of electrically coupled interneurons in the mammalian retina. Neuron *33*, 935–946.

Veruki, M.L., and Hartveit, E. (2009). Meclofenamic acid blocks electrical synapses of retinal AII amacrine and on-cone bipolar cells. J. Neurophysiol. *101*, 2339–2347.

Veruki, M.L., Mørkve, S.H., and Hartveit, E. (2006). Activation of a presynaptic glutamate transporter regulates synaptic transmission through electrical signaling. Nat. Neurosci. *9*, 1388–1396.

Vervaeke, K., Lorincz, A., Nusser, Z., and Silver, R.A. (2012). Gap junctions compensate for sublinear dendritic integration in an inhibitory network. Science *335*, 1624–1628.

Wässle, H., Puller, C., Müller, F., and Haverkamp, S. (2009). Cone contacts, mosaics, and territories of bipolar cells in the mouse retina. J. Neurosci. *29*, 106–117.

Williams, S.R., and Mitchell, S.J. (2008). Direct measurement of somatic voltage clamp errors in central neurons. Nat. Neurosci. *11*, 790–798.